7.3 SERA TA Project #37 – INfills and MASonry structures protected by deformable POLyurethanes in seismic areas (INMASPOL)

Authors

Z. Rakicevic[(1)], A. Bogdanovic[(1)], F. Manojlovski[(1)], A. Shoklarovski[(1)], T. Rousakis[(2)], A. Sapalidis[(2)], A. Ilki[(3)], O. F. Halici[(3)], A. Kwiecień[(4)], A. Viskovic[(5)], F. Rizzo[(5)], M. Kramar[(6)], B. Ghiassi[(7)], A. Benedetti[(8)], C. Colla[(8)], M. Karpała[(9)], K. Agis[(10)], B. Zając[(11)], M. Gams[(12)]

[(1)] *Institute of earthquake engineering and engineering seismology, Ss. Cyril and Methodius University, Skopje, Republic of North Macedonia*

[(2)] *Democritus University of Thrace, Greece*

[(3)] *Istanbul Technical University, Turkey*

[(4)] *Cracow University of Technology (CUT), Poland*

[(5)] *G. D'Annunzio University of Chieti – Pescara, Italy*

[(6)] *Slovenian National Building and Civil Engineering Institute, Ljubljana, Slovenia*

[(7)] *University of Nottingham, UK, University Park Nottingham, UK*

[(8)] *Alma Mater Studiorum-Universita' di Bologna, Italy*

[(9)] *SIKA Poland Sp. z.o.o., Cracow, Poland*

[(10)] *KEBE SA, Head Offices-Factory Nea Santa, Kilkis, Greece*

[(11)] *FlexAndRobust Systems Ltd, Cracow, Poland*

[(12)] *University of Ljubljana (UL), Slovenia*

DOI: 10.7414/SERA-TA.DYNLAB.Project37

7.3.1 Introduction

The behaviour of RC frames with masonry wall infills is influenced a lot by the stiffness and yield displacement difference between the frame and the infill. The flexible frame is unable to carry high loads at low displacements and this can cause the infill to damage already at

moderate seismic intensity. In case of aftershocks, the damaged infills can fail out-of-plane. On the other hand, if the stiff infill is too strong relative to the column, it may cause undesirable behaviour of the frame or even shear failure in the column. The response of structural system can be improved by using a flexible interface between the frame and the infill. This project consisted of testing RC frames with a flexible joint made of polyurethane (PUFJ) with the masonry wall infills. The application of around 2 cm thick PUFJ reduces the stress concentrations at the contact and thereby reduces damage to infills and RC frames and improves the displacement capacity of the structural system. Furthermore, it offers additional amount of damping. Despite the flexibility of the polyurethane (PU), the bond between the PU and the other materials can transfer significant loads during in-plane and out-of-plane excitations. The PUFJ is versatile because different types of PU with very different stiffness, damping and strength characteristics can be used to manipulate the system dynamic behaviour. In case of premature out-of-plane flexural or in-plane diagonal tension infill failure, PUs can be used for bonding of various composite fibres to the weak masonry substrate to form Fiber Reinforced PU (FRPU) as well as for repair of damaged RC frames. The PU can cover emergency situations as it cures within hours and is easy to apply. The proposed project assessed the efficiency of the method through testing of full-scale infilled RC building on shake table. The seismic tests validated in-plane and out-of-plane infill performance when modified, repaired or strengthened with PUFJ and FRPU systems.

7.3.2 Test specimen

The test specimen was fully symmetrical 3D frame RC structure (shown in the Figure 51 and Figure 52) with 4 identical columns with dimensions a/b=20/20cm, reinforced with 8 longitudinal rebars Ø10 and double perpendicular stirrups Ø8/5cm. The beams b/d=20/20 were incorporated in the slab and comprised also od 8 longitudinal rebars Ø10 with single perpendicular stirrups Ø8/5cm. Protective layer of 4.2cm was made, hence the distance from the edge of the element (beam and column) to the centerline of the longitudinal rebars was 5.5cm. The foundation beams intended to fix the model to the shake table were b/d=40/40cm with 10 longitudinal rebars Ø18 with stirrups Ø8/15cm. The slab d=20cm was reinforced with steel rebar nets type Q503. The materials used to construct the bearing elements were concrete C30/37 and rebars B500C.

Infills as non-load bearing masonries were constructed of KEBE Ortho Block K100 system with half bricks at both ends of every second layer using Mounting Mortar M10.

The walls were divided in two types:

- the first parallel pair, type B, built with 2cm gap between the bricks and RC columns and slab. After competition of brick laying procedure, the RC interface was covered with Sika ZP Primer and the gaps were covered with thin longitudinal Sika PS sheets. After the curing process finished then the final step consisting of injection with Sika PUFJ Injection was performed.

- The second parallel walls, type C was built on already glued PUFJ Sika PM laminates on all 4 sides connecting with RC elements (columns, slab and foundation) with cross section b/d=2/10cm.

Figure 51: Completely instrumented and loaded test specimen placed on shake table

7.3.3 Test setup

In general, the experimental investigations were divided in 4 phases:

- phase A, where the walls type B were tested in plane, in direction of the excitation and walls type C were tested out of plane, perpendicular to the direction of excitation.
- Phase A', where only the walls type B were strengthened using GFRPU SikaWrap 350G Grid and SikaPS adhesive.
- Phase B, the specimen was rotated 90 degrees and now, the walls type C were tested in plane and walls type B out of plane.
- Phase B', the walls C were strengthened using the same technique but with tighter sheets.

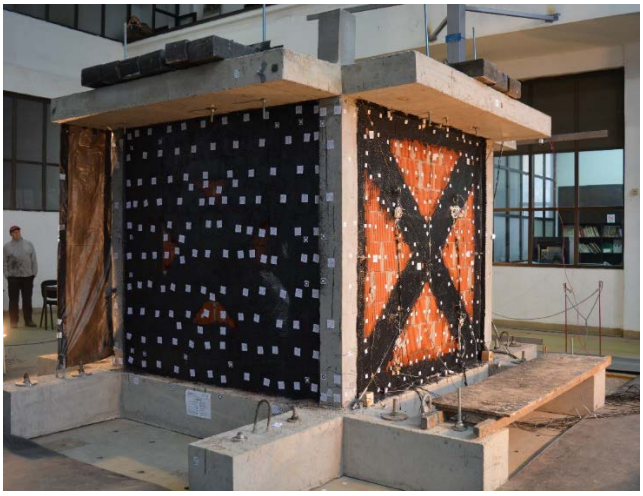

Figure 52: Final phase of tests with strengthening on all walls

The testing methodology consisted of shake table tests for determination of dynamic characteristics of the system by means of white noise and sine sweep low amplitude time histories of acceleration. The focus was on the seismic tests and seismic response of the structure of real earthquake – Chavriata 2014 (Greece) E-W direction with varying intensity, from low amplitude to high amplitude. On the following Figure 53, a time history plot of the maximum tested level of intensity input acceleration is shown. The direction of the excitation in the laboratory is also east – west, as noted by the two-end arrow in the Figure 53 and Figure 54.

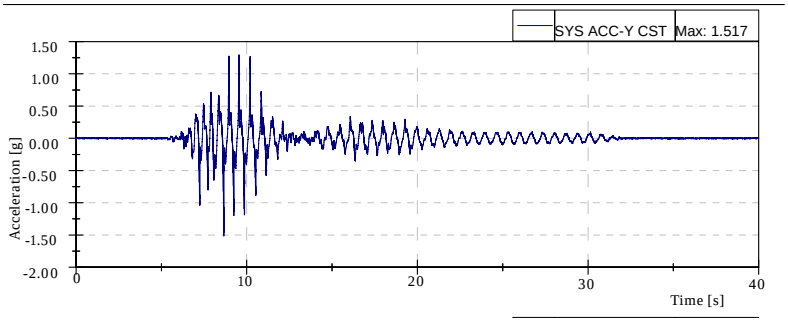

Figure 53: Input acceleration time history for the maximum tested level of intensity

The instrumentation of the tested model comprised of accelerometers (ACC), linear potentiometers (LP) and linear variable differential transformers (LVDT) measuring acceleration, total and relative displacements respectively. Their exact position on every tested setup is clearly shown on the Figure 54 and Figure 55 as well as in the following text.

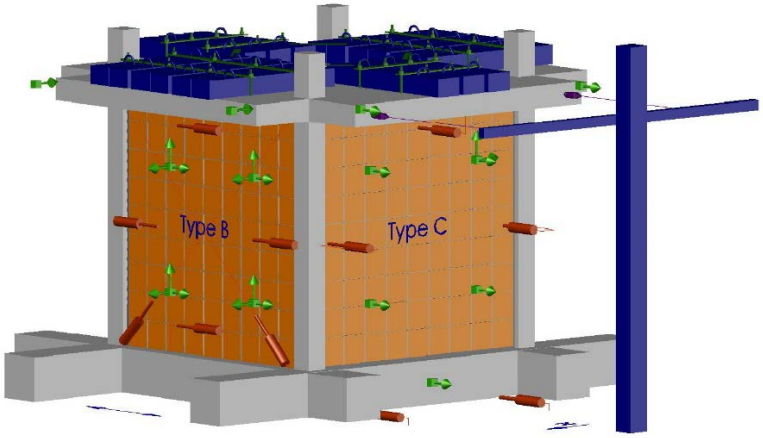

Figure 54: Instrumentation – phase A and A'

The exact location of the transducers in the testing phase A and A' was as follows (note that the only difference is that in phase A' the accelerometers ACC 12, ACC 19 and ACC 20 were detached):

- Ch 1 ACC 1 on the foundation, horizontal dir. (y); Ch 2 ACC 2 on the slab, on the left corner, horizontal dir. (y); Ch 3 ACC 3 on the slab, on the right corner, horizontal dir. (y); Ch 4 ACC 4 on the slab, on the right corner, horizontal dir. (x); Ch 5 ACC 5 on the slab, on the left corner, horizontal dir. (x); Ch 6 ACC 6 on the infill type C, on the lower left side, horizontal dir. (y); Ch 7 ACC 7 on the infill type C, on the lower right side, horizontal dir. (y); Ch 8 ACC 8 on the infill type C, on the upper left side, horizontal dir. (y); Ch 9 ACC 9 on the infill type C, on the upper right side, horizontal dir. (y); Ch 10 ACC 10 on the infill type C, on the upper right side, horizontal dir. (x); Ch 11 ACC 11 on the infill type B, on the lower left side, horizontal dir. (x); Ch 12 ACC 12 on the infill type B, on the lower right side, horizontal dir. (x); Ch 13 ACC 13 on the infill type B, on the upper left side, horizontal dir. (x); Ch 14 ACC 14 on the infill type B, on the upper right side, horizontal dir. (x); Ch 15 ACC 15 on the infill type B, on the upper right side, horizontal dir. (y); Ch 16 ACC 16 on the infill type C, on the upper right side, vertical dir. (z); Ch 17 ACC 17 on the infill type B, on the lower left side, horizontal dir. (y); Ch 18 ACC 18 on the infill type B, on the lower left side, vertical dir. (z); Ch 19 ACC 19 on the infill type B, on the lower right side, horizontal dir. (y); Ch 20 ACC 20 on the infill type B, on the lower right side, vertical dir. (z); Ch 21 ACC 21 on the infill type B, on the upper left side, horizontal dir. (y); Ch 22 ACC 22 on the infill type B, on the upper left side, vertical dir. (z); Ch 23 ACC 23 on the infill type B, on the upper right side, vertical dir. (z); Ch 24 LVDT 1 diagonal, tie slab-foundation, in the direction of excitation; Ch 25 LVDT 2 diagonal, slab-foundation, in the direction of excitation; Ch 26 LVDT 3 foundation-Infill type B, horizontal dir. (y); Ch 27 LVDT 4 RC column-left side of Infill type B, horizontal dir. (y); Ch 28 LVDT 5 RC column-right side of Infill type B, horizontal dir. (y); Ch 29 LVDT 6 RC column-left side of Infill type C, horizontal dir. (y); Ch 30 LVDT 7 slab-Infill type C, horizontal dir. (y); Ch 31 LVDT 8 RC

column-right side of Infill type C, horizontal dir. (y); Ch 32 LVDT 9 on the left side of foundation-Shake table, horizontal dir. (y); Ch 33 LVDT 10 on the right side of foundation-Shake table, horizontal dir. (y); Ch 34 LP1 on the slab, on the left corner, horizontal dir. (y); Ch 35 LP2 on the slab, on the right corner, horizontal dir. (y).

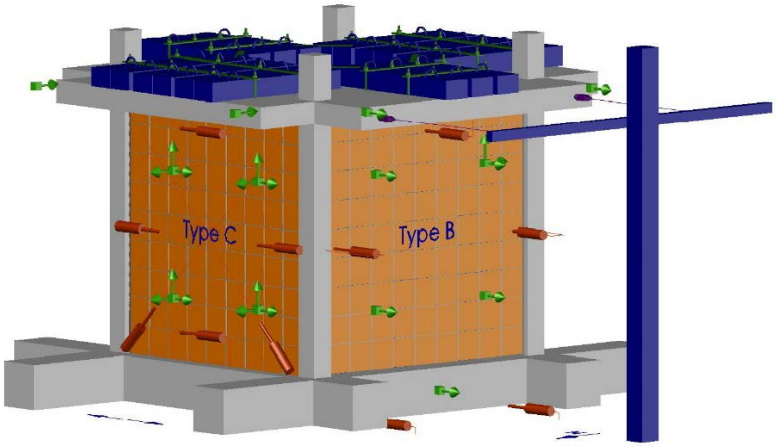

Figure 55: Instrumentation – phase B and B'

The exact location of the transducers in the testing phase B and B' was as follows:

- Ch 1 ACC 1 on the foundation, horizontal dir. (y); Ch 2 ACC 2 on the slab, on the left corner, horizontal dir. (y); Ch 3 ACC 3 on the slab, on the right corner, horizontal dir. (y); Ch 4 ACC 4 on the slab, on the right corner, horizontal dir. (x); Ch 5 ACC 5 on the slab, on the left corner, horizontal dir. (x); Ch 6 ACC 6 on the infill type B, on the lower left side, horizontal dir. (y); Ch 7 ACC 7 on the infill type B, on the lower right side, horizontal dir. (y); Ch 8 ACC 8 on the infill type B, on the upper left side, horizontal dir. (y); Ch 9 ACC 9 on the infill type B, on the upper right side, horizontal dir. (y); Ch 10 ACC 10 on the infill type B, on the upper right side, horizontal dir. (x); Ch 11 ACC 11 on the infill type C, on the lower left side, horizontal dir. (x); Ch 12 ACC 12 on the infill type C, on the lower right side, horizontal dir. (x); Ch 13 ACC 13 on the infill type C, on the upper left side, horizontal dir. (x); Ch 14 ACC 14 on the infill type C, on the upper right side, horizontal dir. (x); Ch 15 ACC 15 on the infill type C, on the upper right side, horizontal dir. (y); Ch 16 ACC 16 on the infill type B, on the upper right side, vertical dir. (z); Ch 17 ACC 17 on the infill type C, on the lower left side, horizontal dir. (y); Ch 18 ACC 18 on the infill type C, on the lower left side, vertical dir. (z); Ch 19 ACC 19 on the infill type C, on the lower right side, horizontal dir. (y); Ch 20 ACC 20 on the infill type C, on the lower right side, vertical dir. (z); Ch 21 ACC 21 on the infill type C, on the upper left side, horizontal dir. (y); Ch 22 ACC 22 on the infill type C, on the upper left side, vertical dir. (z); Ch 23 ACC 23 on the infill type C, on the upper right side, vertical dir. (z); Ch 24 LVDT 1 diagonal, tie slab-foundation, in the direction of excitation; Ch 25 LVDT 2 diagonal, slab-foundation, in the direction of excitation; Ch 26 LVDT 3 foundation-Infill type C, horizontal dir. (y); Ch 27

LVDT 4 RC column-left side of Infill type C, horizontal dir. (y); Ch 28 LVDT 5 RC column-right side of Infill type C, horizontal dir. (y); Ch 29 LVDT 6 RC column-left side of Infill type B, horizontal dir. (y); Ch 30 LVDT 7 slab-Infill type B, horizontal dir. (y); Ch 31 LVDT 8 RC column-right side of Infill type B, horizontal dir. (y); Ch 32 LVDT 9 on the left side of foundation-Shake table, horizontal dir. (y); Ch 33 LVDT 10 on the right side of foundation-Shake table, horizontal dir. (y); Ch 34 LP1 on the slab, on the left corner, horizontal dir. (y); Ch 35 LP2 on the slab, on the right corner, horizontal dir. (y)

On the following Table 13, a complete list of performed dynamic and seismic tests is shown for all 4 phases of testing. Note that the test number follows the internal laboratory numeration of all performed tests

Performed tests							
Test No.	Name	Type of excitation	Intensity	Test No.	Name	Type of excitation	Intensity
PHASE A				PHASE B			
18	Test 2	White noise	0.01g	127	Test 28	White noise	0.01g
20	Test 4	Earthquake	5%	128	Test 29	Earthquake	10%
21	Test 5	Earthquake	10%	129	Test 30	White noise	0.01g
22	Test 6	Earthquake	20%	130	Test 31	Earthquake	20%
23	Test 7	White noise	0.01g	131	Test 32	White noise	0.01g
33	Test 8	Earthquake	40%	148	Test 33	Earthquake	30%
34	Test 9	Earthquake	60%	149	Test 34	White noise	0.01g
35	Test 10	White noise	0.01g	PHASE B’			
36	Test 11	Earthquake	80%	182	Test 35	White noise	0.01g
37	Test 12	White noise	0.01g	183	Test 36	Earthquake	10%
38	Test 13	Earthquake	90%	184	Test 37	White noise	0.01g
39	Test 14	White noise	0.01g	185	Test 38	Earthquake	20%
56	Test 15	Earthquake	90%	186	Test 39	White noise	0.01g
57	Test 16	White noise	0.01g	187	Test 40	Earthquake	30%

58	Test 17	Earthquake	80%	188	Test 41	White noise	0.01g
59	Test 18	White noise	0.01g	189	Test 42	Earthquake	40%
60	Test 19	Earthquake	90%	190	Test 43	White noise	0.01g
PHASE A'				191	Test 44	Earthquake	50%
87	Test 20	White noise	0.01g	192	Test 45	White noise	0.01g
91	Test 24	Earthquake	10%	209	Test 46	Earthquake	60%
92	Test 25	Earthquake	20%	210	Test 47	White noise	0.01g
93	Test 26	Earthquake	30%	211	Test 48	Earthquake	70%
94	Test 27	White noise	0.01g	212	Test 49	White noise	0.01g

Table 13: List of performed shake table tests

7.3.4 Observation during testing

Shake table tests were carried out for various earthquake load levels as explicitly shown in Table 13. In the same time the white noise tests gave insight of the progressive change of the dynamic characteristics of the system. The visual observations during testing as well as direct control of the drifts and change in eigen frequencies, then indirectly the stiffness, led to several major conclusions during testing.

- There was no sliding between the specimen foundations and shake table;
- During the first phase of testing (Phase A) the maximum reached acceleration was 1.64g and there was considerable amount of damages on the walls infill B, while the walls infill C did not experience any out of plane damage;
- The strengthened Phase A' was tested up to only 0.39g due to considerable accumulated damage in the bottom and top joints on the column while the walls were protected by the GFRPU net;
- The rotated specimen on the Phase B was also tested up to 0.35g and then stopped due to the damage on the wall infill C which was later on protected in similar manner as the wall infill type B with GFRPU net;
- Phase B', consisting of all repaired walls was tested up to 0.95g due to fact that the walls were able to withstand horizontal and vertical loads considerably larger then initial setup despite the fact that the RC columns lost a part of its bearing capacity

7.3.5 Results

Shake table tests were carried out for various earthquakes load levels, described in Table 13. Analysis of results were carried out first for horizontal relative displacements of the slab related to the building foundation, measured by two linear potentiometers attached to the support and the shake table displacement (Figure 54 and Figure 55). The relevant drifts of the in-plane tested infills (presented in %) were calculated, assuming their height of 230 cm. Next, changes in eigen-frequencies were analysed.

Setup with wall infills type B tested in-plane (Phase A and A')

In the Phase A, the infills B were tested in-plane in an initial phase up to 90% intensity, where damages of the infills B were hardly observed. During repeated loading by earthquake runs of 90% intensity, the capacity limit state was reached and additional damages in the building occurred due to sudden stop of the shake table, but without visible degradation of the specimen. After checking and correction in the shake table system, the infills B were tested further in the damage phase with 80% and 90% intensity. Formation of significant damages (Figure 60 and Figure 61) were observed during the last one excitation.

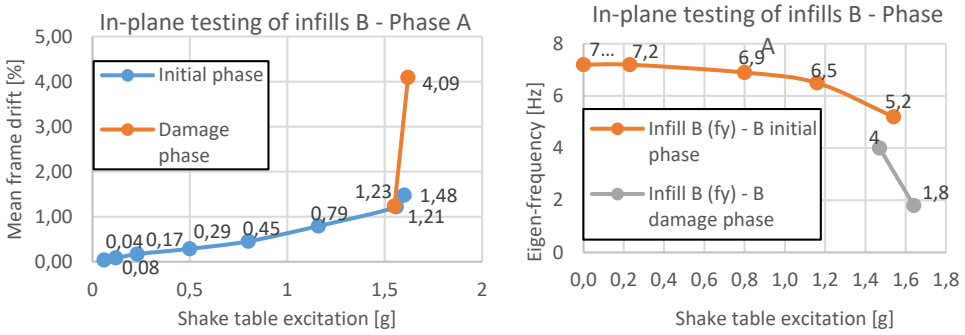

Figure 56: (a) Changes of the drift of the slab (ph. A) (b) Changes of eigen frequency of the str. (ph. A)

Changes in measured maximum horizontal relative displacement of the slab (Y-direction) were used to calculate the RC frame drift using the height of the columns up to the centre of the joint with the beams 240cm (Figure 56a). Observation related to the drift changes are confirmed by the reduction of the main eigen-frequency of the building in the Y-direction from 7.2 Hz to 1.8 Hz, obtained from the random tests (Figure 56b). Significant damages to infills B appeared in the damage phase with 90% intensity. They correspond to reduction of the eigen-frequency below 4 Hz and interfering in resonance with the dominant excitation frequency of the earthquake signal (2.5 - 4.0 Hz).

Almost linear behaviour of the structure was observed up to 60% intensity (1.28 g). The structure started with softening due to the development of plastic hinges in the top and the

bottom of columns and cracks pattern in head and bed mortar joints. Degradation process started with 80% intensity (1.70 g) and was developing when excitation was continuing up to 90% intensity (1.91 g) with meantime repetition of levels 90% and 80%. Drop of main eigen-frequency to 1.8Hz (Figure 56b) and significant damages to the infills B (Figure 60) occurred within 90% intensity excitation, but the structure did not collapse, and no collapse deflection was observed. Moreover, the blocks were kept by the PUFJs on the position with only single blocks rushing out.

The infills B (in such condition) were able to be repaired and strengthened using GFRPU system (Figure 52). After strengthening the infills B, the structure revealed increased eigen-frequency in the Y direction up to 3.6 Hz. After in-plane testing of the strengthened infills B up to 30% (0.64 g) in Phase A', no additional damages were observed, but the eigen-frequency dropped to 2.6 Hz (Figure 57b). Maximum drift obtained during 30% intensity was 1.69% (Figure 57a).

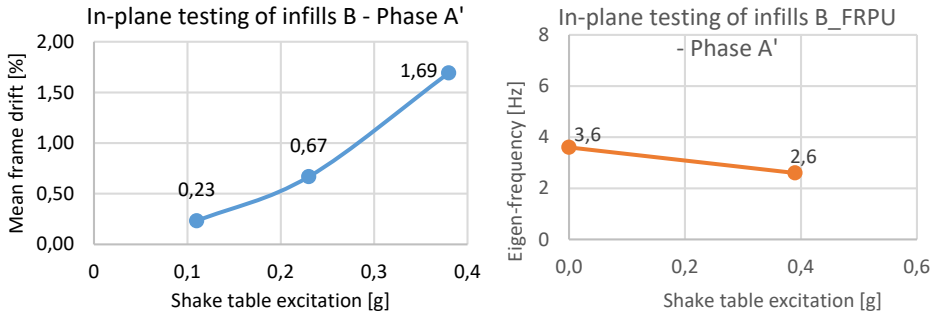

Figure 57: (a) Changes of the drift of the slab (ph. A') (b) Changes of eigen frequency of the str. (ph. A')

The strengthened infills B withstood all out-of-plane earthquake excitations applied to the structure after rotation of the building by 90 degree. The presented results related to the infills B indicate that PUFJ and GFRPU systems effectively protect RC frames and infill walls during strong earthquakes.

Setup with wall infills type C tested in-plane (Phase B and B')

In the Phase A (the infills B tested in-plane), the infills C were tested out-of-plane in the initial phase up to 90% intensity and then in the damage phase with 80% and 90% intensity. Practically no serious damages to the infills C were observed at this stage (only fissures in mortar), as well as after the harmonic resonance test with 16 Hz and 32 Hz frequencies (resonance frequencies of the infills C – out-of-plane moving on PUFJs and bending, respectively). After rotation of the building, the infills C presented slightly non-linear behaviour during in-plane tests. Changes in maximum relative horizontal displacement of the slab and the calculated drift are presented in Figure 58a for the increasing excitation intensity

up to 30%. Observation related to the drift changes are confirmed by small reduction of the eigen-frequency – Figure 58b in the Y-direction: from 3.5 Hz to 2.9 Hz, even if the structure worked in the resonance frequency range of the KEF earthquake excitation (2.5-4.0 Hz).

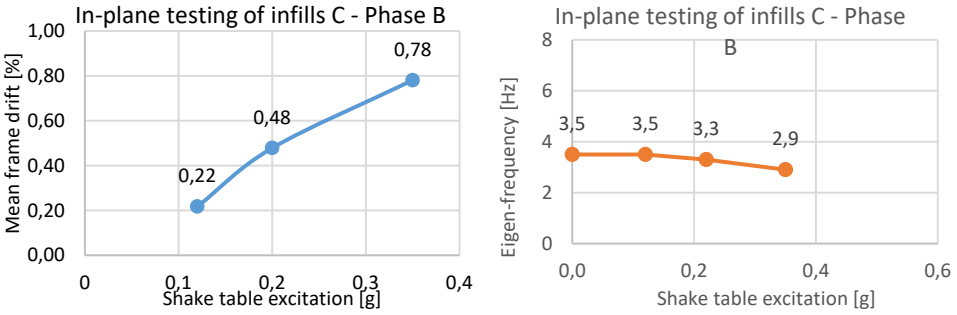

Figure 58: (a) Changes of the drift of the slab (ph. B) (b) Changes of eigen frequency of the str. (ph. B)

In the last phase B', the type C walls were repaired and strengthened using GFRPU system (Figure 52). After strengthening the infills C, the structure revealed increased eigen-frequency in the Y direction up to 5.6 Hz. Strengthened infills C were tested up to 70% (0.95 g) intensity, where the eigen-frequency dropped to 4.6 Hz (Figure 59a). Maximum drift obtained during 70% was 0.99% (Figure 59b).

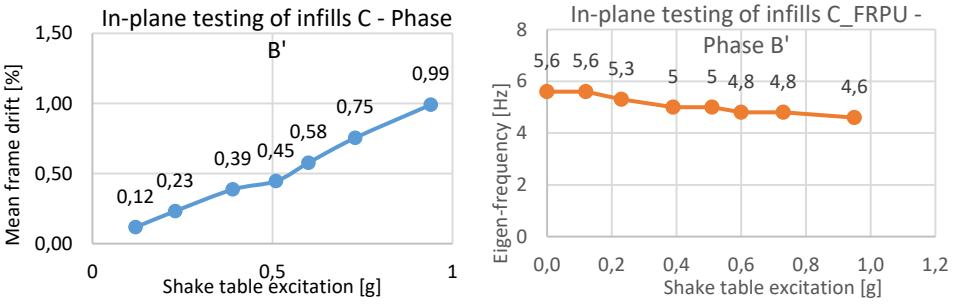

Figure 59: (a) Changes of the drift of the slab (ph. B') (b) Changes of eigen freq. of the str. (ph. B')

Figure 60: Final state of damage – Phase A

Figure 61: Spalled concrete cover of the column in the bottom

7.3.6 Conclusions and outlook

The tests of full-scale structure on a shake table have shown that infills significantly influence the seismic response of the structure. The effects of strong earthquakes on the stiffness and the eigen-frequencies of the structure – both denoting damage accumulation are better controlled in case the ortho block infill-RC frame boundaries are protected with PUFJ joints.

It was observed that due to the flexibility of the 2cm polymer joint, the interaction between the special (KEBE K100) ortho block infill and the RC frame can be manipulated so as to achieve the delay of serious infill damages at very high RC frame inter-storey drifts. The present tests suggest that first brick disintegration (that may cause injuries) occurs at levels far higher than 12% drift while avoiding undesirable effects on the RC columns, caused by the infills. Further, it is validated that the PUFJ protection enables the infill to be strengthened even after very high inter-storey drift of the structure up to 3.8%. Such a level is higher than the one corresponding to repairable damages for RC frames. Therefore, the

PUFJ protected ortho block infill can be effectively transformed to a mechanism remarkably increasing the initial stiffness of the bare RC structure. Secondly, the infill maintains its integrity and bears part of horizontal but most important of vertical loads at high drift levels.

Finally, the applied GFRPU system efficiently protects damaged infills against collapse under out-of-plane excitation while they restore large part of their in-plane stiffness that is countable at RC structure level.

The tests offer direct comparison between joint on three sides (left, top, and right) and joint on all four sides for low excitation levels because of the poor condition of the RC frame after numerous sequential excitations. As expected, a RC structure with ortho block infills protected with polymer joints on all four sides is more flexible in-plane. Both PUFJ systems protect efficiently the ortho block brick in-fills against out of plane failure for very high inter-storey drifts and accelerations. Both PUFJ systems protect the structure with damaged columns against collapse, being able to bear part of the horizontal and vertical load.